

THEORETICAL PREDICTION OF THE GEOMETRIC TRANSFER FUNCTION FOR FOCUSED COLLIMATORS

Charles E. Metz, Ming W. Tsui, and Robert N. Beck

The University of Chicago and The Franklin McLean Memorial Research Institute, Chicago, Illinois

The transfer function describing spatial resolution characteristics of a focused collimator used in conventional scanning can be described by the weighted sum of three terms representing contributions of geometrically collimated, penetrating, and scattered radiation. The present work has shown that the geometric component of the transfer function of a single-hole or multi-hole focused collimator with round holes packed in an hexagonal array can be expressed in the form of a rather simple equation involving trigonometric functions, first-order Bessel functions, and the physical dimensions of the collimator. This expression is applicable for any collimator-to-source distance and takes into account the directional dependence of geometric resolution due to hole-packing geometry. Fourier transformation of line spread functions measured using a thin-walled line source of ^{125}I in air, in which case scatter and septal penetration can be neglected, has shown that the predicted transfer functions are accurate to within a few percent over a broad range of spatial frequencies and collimator-to-source distances. Thus the theoretical approach appears to provide a powerful tool for the designing of focused collimators.

The transfer function of a radiation detector collimator can be described by a linear combination of terms representing geometric unsharpness due to the finite solid angle of acceptance of any hole, penetration unsharpness due to transmission of gamma photons through the collimator septa, and scatter unsharpness due to detection of any X or gamma photons scattered in the radioactive source or surrounding medium (1). The observed collimator transfer function $S(\nu)$ can be written as

$$S(\nu) = [S_g(\nu) + f_p \cdot S_p(\nu) + f_s \cdot S_s(\nu)] / (1 + f_p + f_s) \quad (1)$$

In this expression the terms $S_g(\nu)$, $S_p(\nu)$, and $S_s(\nu)$ represent normalized one-dimensional Fourier transforms of the line spread functions (or two-dimensional Fourier transforms of the point spread functions) due, respectively, to primary photons reaching the detector from the geometric field of view, primary photons penetrating the collimator septa, and any photons reaching the detector after scattering in the source or medium surrounding the source. The terms f_p and f_s represent ratios of the number of penetrating primary photons and any scattered photons detected, respectively, to the number of detected geometrically accepted photons. The geometric component, $S_g(\nu)$, is equivalent to the collimator transfer function observed in the absence of penetration and scatter; this situation can be realized by imaging a thin-walled source in air using an isotope that emits photons of energy sufficiently low so that septal penetration is negligible.

In this paper we show that the geometric component of the transfer function of a single-hole or multihole focused collimator can be expressed rather simply in closed form.

SOURCE IN FOCAL PLANE

For sources in the focal plane, the point spread function describing geometric unsharpness of a single-hole focused collimator with circular apertures is proportional to the fractional area overlap of two disks, each with diameter equal to that of the hole aperture in the collimator back plane, when the centers of the disks are separated by a distance equal to [collimator length] \times [distance of point source from central axis]/[focal length] (2). Equivalently, the fractional overlap can be expressed as that of two disks, each with diameter equal to the radius of view of the hole in the focal plane, when the centers

Received April 17, 1974; revision accepted June 24, 1974.

For reprints contact: Charles E. Metz, Box 429, Dept. of Radiology, The University of Chicago, 950 E. 59th St., Chicago, Ill. 60637.

of the disks are displaced a distance equal to the distance of a point source from the collimator axis.

Since a transfer function is proportional to the two-dimensional Fourier transform of the corresponding point spread function and the fractional overlap of two disks of diameter B can be expressed in terms of the center separation distance ρ by the convolution of two functions $b(x,y)$

$$c(\rho) = \iint_{-\infty}^{\infty} b(x - \rho, y) b(x, y) dx dy \quad (2)$$

where

$$b(x,y) = 1 \quad \text{if } \sqrt{x^2 + y^2} \leq B/2 \quad (3)$$

$$= 0 \quad \text{if } \sqrt{x^2 + y^2} > B/2$$

and since the Fourier transform of the convolution of two functions is given by the product of the transforms of the two functions, one can see that the geometric transfer function for a single-focused collimator hole with a source in the focal plane is proportional to the square of the two-dimensional Fourier transform of the function given in Eq. 3. But the two-dimensional Fourier transform of the function defined by Eq. 3 is proportional to $J_1(\pi\nu B)/\pi\nu B$ where ν represents spatial frequency (cycles per unit length) and the function $J_1(\dots)$ is the first-order Bessel function of the first kind. Thus the geometric transfer function component for a single-focused collimator hole and for sources in the focal plane is given by

$$S_g(\nu) = 4 [J_1(\pi\nu R)/\pi\nu R]^2 \quad (4)$$

after normalization to unity at zero spatial frequency where $R =$ single-hole radius of view. This expression can be rewritten in terms of the dimensions of the collimator hole (2) as

$$S_g(\nu) = 4 [J_1(2\pi r F \nu / L) / (2\pi r F \nu / L)]^2 \quad (5)$$

in which r is hole radius at the back of the collimator, F is collimator face-to-focal plane distance (focal length), and L is collimator length. Values of the function $J_1(\dots)$ are available in tables of functions (3). Referring to Fig. 1 but with the point source in the focal plane ($Z = F$), we remark in passing that the convolution expression for the point spread function—and hence the derived transfer function—is rigorously correct only if the photon flux at any location within a hole in the back plane of the collimator is independent of point source position in the focal plane as long as the point source is within the geometric acceptance “window” at that location. This assumption is satisfied if inverse square and cosine law effects are negligible and hence is satisfied to a good approximation if

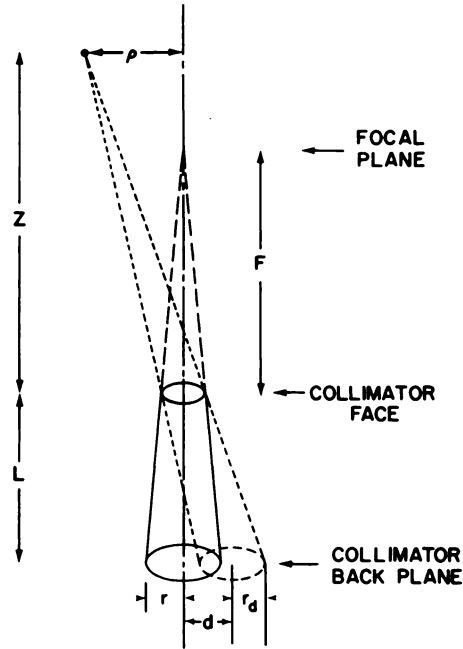


FIG. 1. Geometric relationships among collimator-hole dimensions, point source coordinates, and projection of front-hole aperture onto collimator back plane. Expressions given in text for r_d and d in terms of other parameters shown can be derived using similar triangle arguments.

$$[r/L]^2 [(2F + L)/(F + L)]^2 \ll 1 \quad (6)$$

which is the case for practical collimator designs.

The geometric response of a multihole focused collimator used in conventional scanning is given by the sum of the geometrical responses of the individual holes. If all holes are focused on the same point and if all hole apertures are circular and of the same size, then one can show that the fields of view of all holes coincide in the focal plane. Thus in this case Eqs. 4 and 5 describe the transfer function corresponding to geometric unsharpness of the multihole collimator for sources in the focal plane if the array of holes is small enough so that a uniformity condition analogous to condition 6 is satisfied for the off-axis, slanted holes. Alternatively, if all holes are focused on the same point but if all hole cross sections perpendicular to the hole axes are circular and of the same size at a given distance from the focal point (as is often the case for practical multihole collimators), then again Eqs. 4 and 5 are valid only for a restricted range of overall diameters of the array of holes since the fields-of-view of off-axis, sharply slanted holes are increased for large arrays. In both cases, the expressions given above should be valid to a good approximation if the largest distance between hole centers in the collimator back plane, D_c , is small enough so that

$$D_c^2 / 4 (F + L)^2 \ll 1 \quad (7)$$

which is the case for most practical multihole focused collimators and if condition 6 is satisfied for each hole.

SOURCE OUT OF FOCAL PLANE:
SINGLE-HOLE CASE

Using arguments similar to those for the case of a point source in the focal plane, one can show that, for the case of a point source not necessarily in the focal plane, the point spread function describing geometric unsharpness for a single-hole focused collimator with circular apertures is proportional to the fractional overlap or convolution of two disks of generally unequal diameters. For this more general case, the appropriate disk diameters are proportional to the diameter of the back collimator aperture and to the diameter of the projection of the front collimator aperture onto the back collimator plane from the point source located a distance Z from the collimator face. One can see from Fig. 1 that the appropriate disk diameters are $2r$ and $2r_d = 2rF(L + Z)/[Z(L + F)]$, respectively, and that the displacement d between disk centers for a point source displaced a distance ρ from the central axis and a distance Z from the collimator face is given by $\rho L/Z$.

Thus the point spread function for a point source located a distance Z from the collimator face, expressed in terms of point source position ρ , is proportional to the convolution of two disks of diameters $2rZ/L$ and $2rF(L + Z)/L(L + F)$. The corresponding geometric unsharpness transfer function for a single tapered hole is given by the product of the two-dimensional Fourier transforms of the two disks normalized to unity at zero spatial frequency so that

$$S_{g^{s.h.}}(\nu) = 4 \left(\frac{J_1\{(2\pi r F \nu / L)[(L + Z)/(L + F)]\}}{(2\pi r F \nu / L)[(L + Z)/(L + F)]} \right) \left(\frac{J_1(2\pi r Z \nu / L)}{2\pi r Z \nu / L} \right) \quad (8)$$

for a source in a plane located a distance Z from the collimator face. For this more general case, the constraint for applicability of the convolution ap-

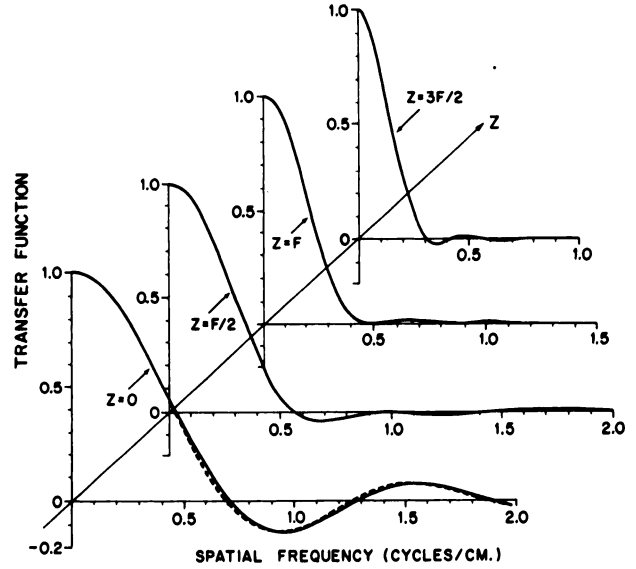


FIG. 2. Predicted (solid curves) and observed (dotted curves) geometric transfer functions for single-hole collimator studied. Where only solid line is shown, predicted and observed curves are graphically indistinguishable.

proach and hence of the transfer function result remains that given by condition 6. For sources in the focal plane, $Z = F$, and Eq. 8 reduces to Eq. 5.

SOURCE OUT OF FOCAL PLANE:
MULTIHOLE CASE

For the general case of a multihole focused collimator viewing a source not in the focal plane, the fields of view of the individual holes do not coincide, and thus the field-of-view of the array of holes is larger than that of any individual hole. In this case, the geometric response point-spread function of the array of holes is proportional to an array of geometric response point spread functions, each due to an individual hole.

If the largest distance between hole centers in the collimator back plane, D_c , is small enough so that condition 7 is satisfied, then the point spread functions due to the various holes will be of essentially the same shape. Thus the point spread function of the array of holes is proportional to an appropriately

	1	19	37
Number of holes	1	19	37
Length (L) [cm]	10.16	6.75	6.47
Hole radius in back plane (r) [cm]	2.54	0.42	0.40
Focal length (F) [cm]	5.18	10.16	7.62
Hole array type	—	Complete hexagonal	Complete hexagonal
Hole center separation in back plane [cm]	—	0.953	1.135
Geometric efficiency [cm ²]	3.61×10^{-3}	3.75×10^{-3}	5.41×10^{-3}

* All collimators are made of lead with round hole cross sections perpendicular to hole axes.

scaled array of similar point spread functions, each equal to that due to a single hole. Since an array of similar functions can be expressed mathematically by convolution of the function with an array of appropriately spaced "impulse" functions, the transfer function of the array of holes is proportional to the product of the single-hole transfer function for the source plane-collimator face distance in question and the two-dimensional Fourier transform of the appropriately scaled array of impulse functions.

The normalized two-dimensional Fourier transform of a complete hexagonal array of impulse functions with $(M + 1)$ points on a side, the points being spaced a distance s apart, and with a vertex on the y -axis is given by

$$H_M(\nu, \theta; s) = \frac{1}{[1 + 3M(M + 1)][\cos \alpha - \cos \beta]} \cdot \left\{ \begin{aligned} &\cos [(M + 1)\alpha] \sin [(M + 1)\beta] / \sin \beta \\ &- \cos [M\alpha] \sin [M\beta] / \sin \beta \quad (9) \\ &- \cos [(2M + 1)\beta] \end{aligned} \right.$$

with $\alpha \equiv \sqrt{3}\pi s \nu \cos \theta$ and $\beta \equiv \pi s \nu \sin \theta$ for $\theta \neq 0, \pm 60^\circ$, or $\pm 120^\circ$. For $\theta = 0, \pm 60^\circ$, or $\pm 120^\circ$, however, the transform of the array is given by

$$H_M(\nu, \theta; s) = \frac{1}{[1 + 3M(M + 1)][1 - \cos(\sqrt{3}\pi s \nu)]} \cdot \left\{ \begin{aligned} &1 + M \cos [M\sqrt{3}\pi s \nu] \quad (10) \\ &- (M + 1) \cos [(M + 1)\sqrt{3}\pi s \nu] \end{aligned} \right.$$

In these expressions, the angle θ can be interpreted as the angle with which a line source used to measure a line spread function intersects a side of the hexagonal array when the line source passes over the center of the array and thus it can be restricted to the range $60^\circ \leq \theta \leq 90^\circ$ [i.e., $\pi/3 \leq \theta \leq \pi/2$ radians]. One can show that expressions 9 and 10 approach unity in the limit as $\nu \rightarrow 0$ or $s \rightarrow 0$.

Thus the geometric component of the transfer function of a multihole collimator with holes in a complete hexagonal array is given by the expression

$$S_g^{m,h}(\nu) = S_g^{s,h}(\nu) \cdot H_M(\nu, \theta; s) \quad (11)$$

The first term on the right is the single-hole transfer function given by Eq. 8. The second term on the right is given by Eq. 9 or 10 in which M is one less than the number of holes on a side of the border of the array* and $s = [D_c(Z - F)]/[2M(L + F)]$ is the distance between hole centers (i.e., single-hole point spread function centers) scaled to the source plane-collimator face distance Z in question. This geometric transfer function of the multihole collimator

* The total number of holes in such a complete hexagonal array is given by $1 + 3M(M + 1)$.

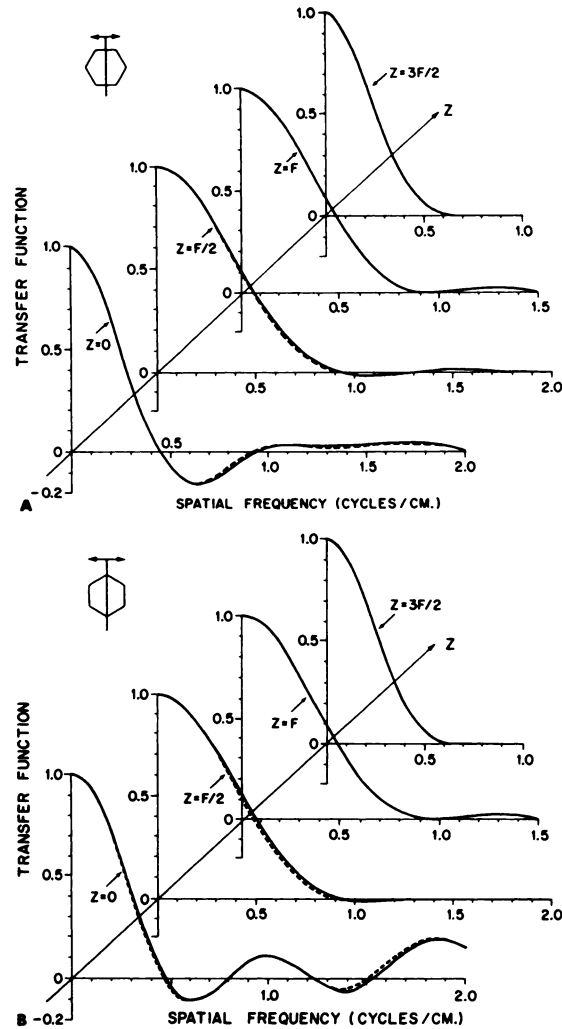


FIG. 3. Predicted (solid curves) and observed (dotted curves) geometric transfer functions for 19-hole collimator studied. Where only solid line is shown, predicted and observed curves are graphically indistinguishable. Upper left insets show life source orientation relative to hexagonal hole-packing geometry. (A) Line source perpendicular to side of hexagonal ring of holes when over center hole ($\theta = 90^\circ$). (B) Line source over vertex of hexagonal ring of holes when over center hole ($\theta = 60^\circ$).

depends on the orientation angle θ since the hexagonal array of hole causes the measured line spread function to depend in general upon the orientation of the line source. This angular dependence is usually small, however, except for sources close to the collimator face.

COMPARISON WITH EXPERIMENT

The transfer function of a focused collimator can be measured by using the collimator with a radiation detector to scan perpendicular to a line source of radioactivity, normalizing the resulting relative radiation intensity data to yield the collimator line spread function and Fourier transforming the line spread function using a digital computer (4,5). If the measurement is made under conditions for which

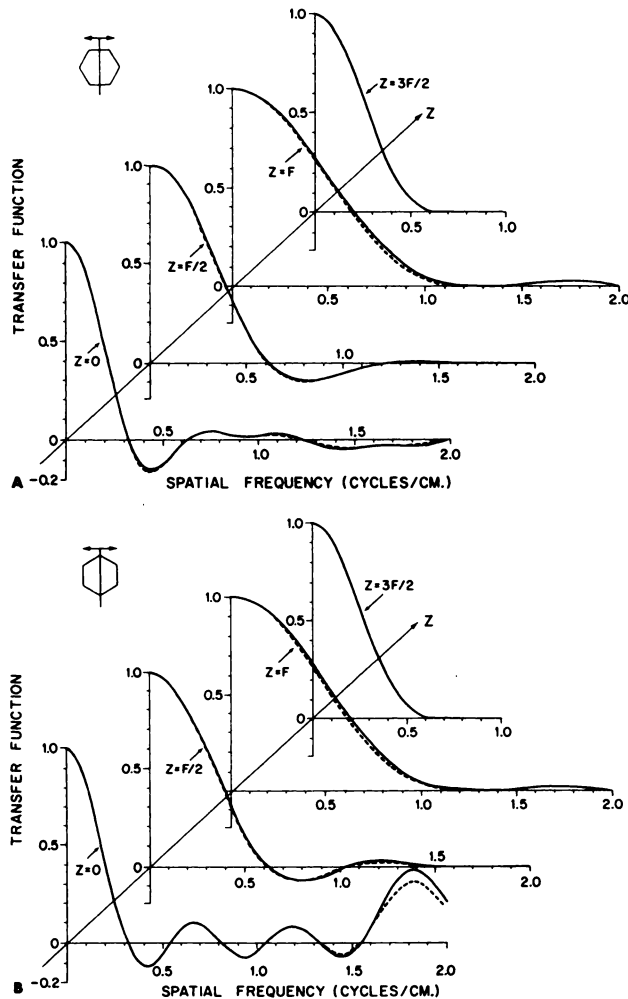


FIG. 4. Predicted (solid curves) and observed (dotted curves) geometric transfer functions for 37-hole collimator studied. Where only solid line is shown, predicted and observed curves are graphically indistinguishable. Upper left insets show line source orientation relative to hexagonal hole-packing geometry. (A) Line source perpendicular to side of hexagonal ring of holes when over center hole ($\theta = 90^\circ$). (B) Line source over vertex of hexagonal ring of holes over center hole ($\theta = 60^\circ$).

both scattered and septa-penetrating radiations recorded by the detector are negligible, then the resulting transfer function is equivalent to the geometric component computed above.

Line spread functions and resulting transfer functions were measured for the three focused collimators described in Table 1 by scanning a 10-cm-long* thin-walled (polyethylene tube; 0.35 mm i.d.; 1.05 mm o.d.) line source of ^{125}I in air using a 3-in. diam, 0.5-in. thick NaI(Tl) radiation detector and a 20–50-keV pulse-height window setting to record pho-

* Although a 30-cm-long line source is generally recommended when scatter and/or penetration are present, we found the 10-cm-long source to be sufficient for these experiments since both scatter and penetration are negligible, and since the 10-cm-long source covered the geometric fields of view for the collimators and source-to-collimator distances studied.

tons from the principal 27.4 and 35-keV lines of the ^{125}I spectrum. Because the mean free path of 35-keV photons in lead is only about 0.06 mm, the scattered and septa-penetrating radiation recorded by the detector could be considered to be negligible. Hence, the measured transfer functions should agree with the predictions of Eq. 11.

To minimize errors in the measured transfer functions due to sampling (6), truncation (7), and statistical fluctuations (8) in the measured line spread function the line-spread function data were sampled at 0.127-mm intervals, “tails” of the line spread function data were observed until the net value fell to 0.1% of the maximum net value, and the scanning speed was adjusted to yield a total of approximately 2×10^6 net detected counts for each line spread function measurement.

Figure 2 shows predicted and observed geometric transfer functions for the single-hole collimator studied with sources placed against the collimator face and at distances of 0.5, 1.0, and 1.5 times the focal length. Differences between the predicted and observed transfer function values are too small to be demonstrated graphically except with the source against the collimator face. Since this collimator consists of a single round hole, the line spread functions and hence the transfer functions do not depend upon line source orientation.

Figures 3 and 4 show predicted and observed geometric transfer functions for the 19-hole and 37-hole collimators studied, respectively, for two different orientations of the line source. Although small differences between the predicted and observed transfer functions can be noted in some cases, agreement is excellent over the range of spatial frequencies and collimator-to-source distances studied and no trend toward disagreement is apparent. Because of the experimental precision required for the measurement of transfer functions to within a few percent, the small differences observed cannot be clearly ascribed either to errors in prediction or errors in measurement.

DISCUSSION

The approach taken here can be generalized to include cases in which hole apertures are noncircular and in which hole arrays are nonhexagonal. For non-circular hole apertures, the function $2J_1(\dots)/(\dots)$ can be replaced by the normalized two-dimensional Fourier transform of the appropriate hole aperture transmission function. Similarly, for hole arrays other than complete hexagonal, the function $H_M(\nu, \theta; s)$ can be replaced by the Fourier transform of an appropriate array of impulse functions.

The excellent agreement between predicted and measured transfer function geometric components for the collimators studied suggests that the approach provides a powerful tool for the designing of focused collimators.

ACKNOWLEDGMENTS

This work was supported in part by The Center for Radiologic Image Research, Department of Radiology, The University of Chicago (USPHS Grant GM-18940) and in part by The Franklin McLean Memorial Research Institute, which is operated by the University of Chicago for the USAEC.

REFERENCES

1. BECK RN: The scanning system as a whole. In *Fundamental Problems in Scanning*, Gottschalk A, Beck RN, eds, Springfield, Ill, Charles C Thomas, 1968, pp 17-39
2. BECK RN: Collimation of gamma rays. In *Fundamental Problems in Scanning*, Gottschalk A, Beck RN, eds, Springfield, Ill, Charles C Thomas, 1968, pp 71-92
3. OLVER FWJ: Bessel functions of integer order. In

Handbook of Mathematical Functions, Abramowitz M, Stegun IA, eds, Washington, DC, National Bureau of Standards, 1968, pp 355-433

4. MACINTYRE WJ, FEDORUK SO, HARRIS CC, et al: Sensitivity and resolution in radioisotope scanning: A report to the International Commission on Radiation Units and Measurements. In *Medical Radioisotope Scintigraphy*, vol 1, Vienna, IAEA, 1969, pp 391-435

5. HINE GJ, TSIALAS SP: Evaluation of focused collimator performance. III. Three- and five-inch-diameter collimators for ¹²⁵I and ^{99m}Tc. In *Medical Radioisotope Scintigraphy*, vol 1, Vienna, IAEA, 1969, pp 487-507

6. METZ CE, STRUBLER KA, ROSSMANN K: Choice of line spread function sampling distance for computing the MTF of radiographic screen-film systems. *Phys Med Biol* 17: 638-647, 1972

7. DOI K, STRUBLER KA, ROSSMANN K: Truncation errors in calculating the MTF of radiographic screen-film systems from the line spread function. *Phys Med Biol* 17: 241-250, 1972

8. METZ CE: A mathematical investigation of radioisotope scan image processing. Doctoral thesis, University of Pennsylvania, 1969. Ann Arbor, Mich., University Microfilms, Publication 70-16,186, pp 211-216